Charged hadron transverse momentum distributions in Au+Au collisions at $\sqrt{s_{NN}} = 200$ GeV

B.B.Back[1], M.D.Baker[2], D.S.Barton[2], R.R.Betts[6], M.Ballintijn[4], A.A.Bickley[7], R.Bindel[7], A.Budzanowski[3], W.Busza[4], A.Carroll[2], M.P.Decowski[4], E.García[6], N.George[1,2], K.Gulbrandsen[4], S.Gushue[2], C.Halliwell[6], J.Hamblen[8], G.A.Heintzelman[2], C.Henderson[4], D.J.Hofman[6], R.S.Hollis[6], R.Hołyński[3], B.Holzman[2], A.Iordanova[6], E.Johnson[8], J.L.Kane[4], J.Katzy[4,6], N.Khan[8], W.Kucewicz[6], P.Kulinich[4], C.M.Kuo[5], W.T.Lin[5], J.W.Lee[4], S.Manly[8], D.McLeod[6], A.C.Mignerey[7], R.Nouicer[6], A.Olszewski[3], R.Pak[2], I.C.Park[8], H.Pernegger[4], C.Reed[4], L.P.Remsberg[2], M.Reuter[6], C.Roland[4], G.Roland[4], L.Rosenberg[4], J.Sagerer[6], P.Sarin[4], P.Sawicki[3], W.Skulski[8], S.G.Steadman[4], P.Steinberg[2], G.S.F.Stephans[4], A.Sukhanov[2], J.-L.Tang[5], R.Teng[8], A.Trzupek[3], C.Vale[4], G.J.van Nieuwenhuizen[4], R.Verdier[4], G.I.Veres[4], B.Wadsworth[4], F.L.H.Wolfs[8], B.Wosiek[3], K.Woźniak[3], A.H.Wuosmaa[1], B.Wysłouch[4]

[1] Argonne National Laboratory, Argonne, IL 60439-4843, USA
[2] Brookhaven National Laboratory, Upton, NY 11973-5000, USA
[3] Institute of Nuclear Physics, Kraków, Poland
[4] Massachusetts Institute of Technology, Cambridge, MA 02139-4307, USA
[5] National Central University, Chung-Li, Taiwan
[6] University of Illinois at Chicago, Chicago, IL 60607-7059, USA
[7] University of Maryland, College Park, MD 20742, USA
[8] University of Rochester, Rochester, NY 14627, USA

(Dated: June 8, 2006)

We present transverse momentum distributions of charged hadrons produced in Au+Au collisions at $\sqrt{s_{NN}} = 200$ GeV. The spectra were measured for transverse momenta p_T from 0.25 to 4.5 GeV/c in a rapidity range of $0.2 < y_\pi < 1.4$. The evolution of the spectra is studied as a function of collision centrality, from 65 to 344 participating nucleons. The results are compared to data from proton-antiproton collisions and Au+Au collisions at lower RHIC energies. We find a significant change of the spectral shape between proton-antiproton and peripheral Au+Au collisions. Comparing peripheral to central Au+Au collisions, we find that the yields at high p_T exhibit approximate scaling with the number of participating nucleons, rather than scaling with the number of binary collisions.

The yield of charged hadrons produced in collisions of gold nuclei at an energy of $\sqrt{s_{NN}} = 200$ GeV has been measured with the PHOBOS detector at the Relativistic Heavy-Ion Collider (RHIC) at Brookhaven National Laboratory. The data are presented as a function of collision centrality and transverse momentum p_T. The goal of our measurements is to test our understanding of Quantum Chromodynamics (QCD), the fundamental theory of the strong interaction. Using nuclear collisions, QCD can be studied in a regime of high temperature and energy density. Calculations suggest [1] that under these conditions a new state of matter, the quark-gluon plasma, will be formed.

In the theoretical analysis of particle production in hadronic and nuclear collisions, a distinction is often made between the relative contributions from "hard" parton-parton scattering processes and "soft" processes. The former can be calculated using perturbative QCD, whereas the latter are typically treated by phenomenological models that describe the non-perturbative sector of QCD [2]. The contribution from hard processes is expected to grow with increasing collision energy and to dominate particle production at high transverse momenta. Collisions of heavy nuclei offer ideal conditions to test our understanding of this picture, as "hard" processes are expected to scale with the number of binary nucleon-nucleon collisions N_{coll}, whereas "soft" particle production is expected to exhibit scaling with the number of participating nucleons N_{part}. In Glauber-model calculations, N_{coll} scales approximately as $(N_{part})^{4/3}$. For central collisions of Au nuclei, this leads to an increase of a factor of six in the ratio of N_{coll}/N_{part}, relative to proton-proton collisions. Collision centrality is therefore a parameter by which the relative contributions of hard and soft processes to particle production can be varied. It was found that a description based on a combination of hard and soft particle production is compatible with the observed centrality dependence of the charged particle multiplicity at mid-rapidity in Au+Au collisions [3, 4], although the result can also be described by models which incorporate initial state parton saturation [5]. A simultaneous study of the p_T and centrality dependence of particle yields may allow us to better discriminate between these different physical pictures.

For Au+Au collisions at RHIC energies, it has been predicted that the yield and momentum distribution of particles produced by hard scattering processes may be modified by "jet quenching", *i.e.* the energy loss of high momentum partons in the dense medium [6]. This phenomenon has been proposed as a diagnostic tool for characterizing the parton density in the initial stage of high-energy nuclear collisions. First results for central Au+Au collisions at $\sqrt{s_{NN}} = 130$ GeV have shown that particle spectra at large transverse momenta indeed change in comparison to p+p collisions [7]. This result has been used to estimate the energy loss in the dense medium [8]. However, calculations have not yet shown a consistent interpretation of the data on spectral shapes and particle multiplicities. The latter seem to be overpredicted [9] when the effects of jet quenching are included. Here we probe the scaling of particle production over a wide range of N_{coll} and N_{part} in different regimes of p_T that are traditionally believed to be dominated by soft or hard processes.

The data were collected using the PHOBOS two-arm magnetic spectrometer [10, 11, 12]. The spectrometer arms are each equipped with 16 layers of Silicon sensors, providing charged particle tracking both outside and inside the 2 T field of the PHOBOS magnet. Particles within the geometrical acceptance region used in this analysis traverse at least 14 of the layers. A two layer silicon vertex detector covering $|\eta| < 0.92$ and 25% of the azimuthal angle provided additional information on the position of the primary collision vertex. In total, 135168 detector elements were read out, of which less than 2% were non-functional.

The primary event trigger was provided by two sets of 16 scintillator paddle counters covering pseudorapidities $3 < |\eta| < 4.5$. Additional information for event selection was obtained from two zero-degree calorimeters which detect spectator neutrons. Details of the event selection and centrality determination can be found in [4, 13]. Monte Carlo (MC) simulations of the apparatus were based on the HIJING event generator [14] and the GEANT 3.21 simulation package, folding in the signal response for scintillator counters and silicon sensors.

For this analysis, the events were divided into six centrality classes, based on the observed signal in the paddle counters. Given the monotonic relationship between the multiplicity of produced particles in the paddle acceptance and the number of participating nucleons $\langle N_{part} \rangle$, the results of a Glauber-model calculation were used [4, 13] to estimate the average number of participating nucleons and the number of binary collisions for each centrality class. The resulting values are shown in Table I.

As the geometrical layout of the PHOBOS detector leads to an asymmetry in the acceptance and detection efficiency for positively and negatively charged particles for a given magnet polarity, data were taken using both polarities. The reproducibility of the absolute field strength was found to be better than 1%, based on Hall probe measurements for each polarity and the comparison of mass distributions for identified particles at the two polarities.

To optimize the precision of the vertex and track finding, only events with a reconstructed primary vertex position between -10 cm $< z_{vtx} <$ 10 cm along the beam axis were selected. By requiring a consistent vertex position from the spectrometer and vertex subdetectors, in combination with the known position of the beam orbit, a vertex resolution better than 0.3 mm (RMS) in the longitudinal and vertical directions, z and y, and better than 0.5 mm in the horizontal direction, x, was achieved.

Details of the reconstruction algorithm for particle tracks can be found in [15]. Track candidates were found combining a road-following algorithm in the region outside the magnetic field and a transformation algorithm for pairs of hits inside the field. The distance of closest approach of each reconstructed track with respect to the primary vertex (d_{vtx}) was used to reject background particles from decays and secondary interactions. The final track selection was based on the χ^2 fit probability of a full track fit, taking into account multiple scattering and energy loss. For further analysis, particles with a rapidity of $0.2 < y_\pi < 1.4$ were used, assuming the pion mass for calculating y_π.

To obtain the invariant yield for charged hadrons, the observed transverse momentum distributions were corrected for the geometrical acceptance of the detector, the efficiency of the tracking algorithm and the distortion due to binning and momentum resolution. For the acceptance and efficiency corrections, the correction factors in p_T and y vary as a function of vertex position and are different for the two charge signs in a given field polarity. The correction factors were obtained in vertex bins of ± 2.5 cm size by embedding the same MC particle tracks into "empty" events and data events. The events were reconstructed with the standard reconstruction chain with and without the additional embedded tracks. From this comparison, a correction factor as a function of p_T and multiplicity was extracted. Over the centrality range covered in this analysis, the reconstruction efficiency decreased by approximately 10%.

MC-simulations based on HIJING and GEANT were used to obtain correction factors for the contribution of secondary particles to the charged particle spectra. The acceptance for secondary and feeddown particles is limited to those produced within 10 cm radial distance

from the primary collision vertex, as accepted tracks were required to have at least one hit in the first two layers of the spectrometer. The background contamination is further reduced by requiring the particle tracks to have $d_{vtx} < 3.5$ mm. We found that the contamination varies from less than 4% at $p_T \approx 0.3$ GeV/c to less than 2% at $p_T > 2.5$ GeV/c. The corresponding correction was applied independent of collision centrality.

The contamination by wrongly reconstructed ("ghost") tracks was studied using two methods. The reconstruction of HIJING events showed a rate of ghost tracks after all quality cuts of less than 4% at $p_T \approx 0.5$ GeV/c and less than 2% at $p_T \approx 2.5$ GeV/c. At higher p_T, the available MC statistics did not allow a precise determination of the ratio of ghost tracks to found tracks. However, MC simulations showed that most ghost tracks arise from a wrong match of track segments inside and outside the magnetic field. The rate of accidental matches was tested by swapping straight and curved track segments between the two spectrometer arms. We found a contribution of accidental matches of less than 1% in the $p_T > 3$ GeV/c region.

Finally, the spectra were corrected for the effects of the finite bin-width and the momentum resolution using an iterative procedure. The resolution was determined using track embedding and the full reconstruction and fitting procedure. For embedded MC tracks we found a momentum resolution of $\Delta p/p = 1 - 9\%$ for the momentum range of 0.3 to 10 GeV/c. The corresponding correction was performed for each centrality bin separately, taking into account the non-Gaussian tails in the p_T-resolution function. At $p_T \approx 4$ GeV/c, the correction varies from a factor of 0.92 for the most peripheral events to 0.89 for the most central events.

Centrality	N_{events}	$\langle N_{part} \rangle$	$\langle N_{coll} \rangle$
45-50%	593942	65 ±4	107
35-45%	1196402	93 ±5	175
25-35%	1192357	138 ±6	300
15-25%	1193373	200 ±8	500
6-15%	1057007	276 ±9	780
0-6%	604555	344 ±11	1050

TABLE I: Details of the centrality bins used. The estimated uncertainty in $\langle N_{coll} \rangle$ ranges from 15% to 10% going from the most peripheral to the most central bin.

In Fig. 1 we show the invariant yield of charged hadrons as a function of transverse momentum, obtained by averaging the yields of positive and negative hadrons. Data are shown for 6 centrality bins, ranging from $\langle N_{part} \rangle = 65$ to $\langle N_{part} \rangle = 344$. The integrated yields, when scaled by $\langle N_{part} \rangle$, increase by 15% over the centrality range, consistent with the centrality evolution of the mid-rapidity particle density presented in [4].

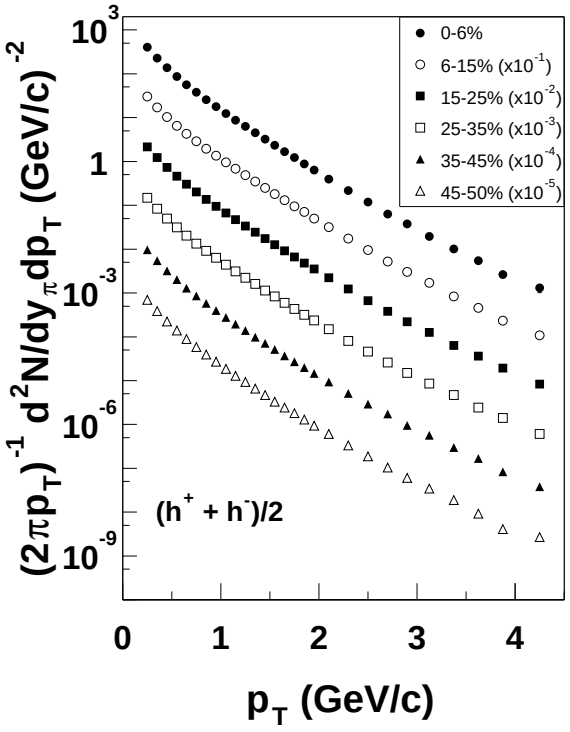

FIG. 1: Invariant yields for charged hadrons as a function of p_T for 6 centrality bins. For clarity, consecutive bins are scaled by factors of 10. Statistical and systematic uncertainties are smaller than the symbol size.

In Fig. 2 we show the ratios of data for the most peripheral bin ($\langle N_{part} \rangle = 65 \pm 4$) and the most central bin ($\langle N_{part} \rangle = 344 \pm 11$) to a fit of the measured p_T-distribution in proton-antiproton collisions at the same energy [16]. In both cases, the Au+Au data were divided by the respective value of $\langle N_{part}/2 \rangle$. The brackets indicate the systematic uncertainty in the Au+Au data (90% C.L.). The largest contribution to the systematic uncertainty are the overall tracking efficiency, independent of p_T, and the p_T dependent momentum resolution and binning correction. The small contamination by secondary particles and feeddown particles, due to the proximity of the tracking detectors to the collision vertex, also ensures that the uncertainty in the corresponding correction factors is small. Similarly, the high granularity and resolution of the tracking planes leads to small uncertainty in the rate of 'ghost' tracks.

As has been shown previously [9, 13], the yield per participant pair in Au+Au collisions at these centralities is significantly larger than in proton-antiproton collisions

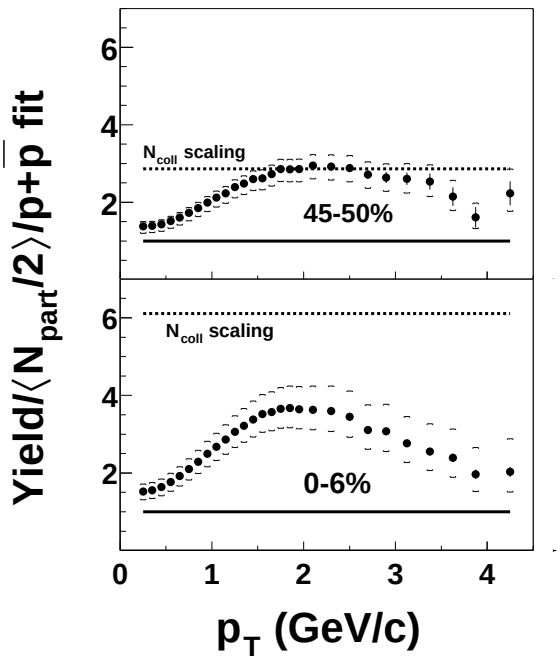

FIG. 2: Ratio of the yield of charged hadrons as a function of p_T for the most peripheral bin ($\langle N_{part}\rangle = 65 \pm 4$, upper plot) and the most central bin ($\langle N_{part}\rangle = 344 \pm 11$, lower plot) to a fit of proton-antiproton data (see text) scaled by $\langle N_{part}/2\rangle$. The dashed (solid) line shows the expection of N_{coll} (N_{part}) scaling relative to $p + \bar{p}$ collisions. The brackets show the systematic uncertainty of the Au+Au data.

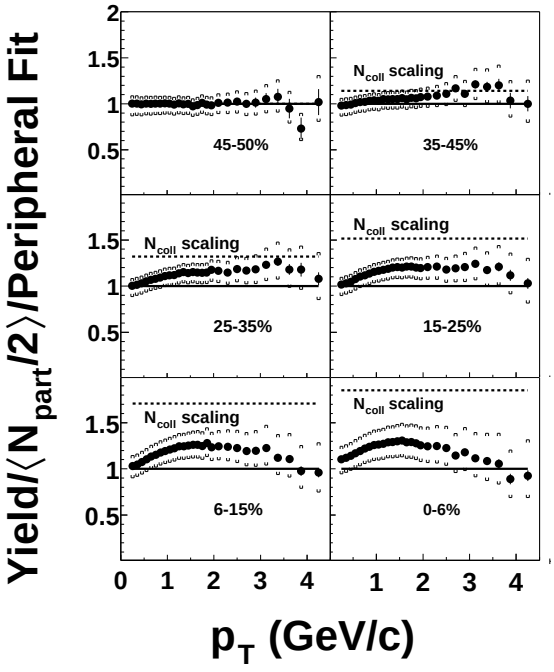

FIG. 3: Charged hadron yield in Au+Au in six centrality bins, divided by a fit to the most peripheral bin and by $\langle N_{part}/2\rangle$. The dashed (solid) line shows the expectation for N_{coll} (N_{part}) scaling relative to peripheral collisions. The brackets show the systematic uncertainty in the Au+Au data.

at the same energy. We also observe that in peripheral Au+Au collisions with $\langle N_{part}\rangle = 65$, corresponding to an impact parameter $b \approx 10$ fm, the spectral shape is already strongly modified from that in $p+\bar{p}$ collisions. It is worth noting that the ratio $\frac{\langle N_{coll}\rangle}{\langle N_{part}/2\rangle}$ increases by a factor of almost three from $p + \bar{p}$ to the most peripheral Au+Au collisions studied here. For the highest p_T, the yield for central events is significantly smaller than expectations based on N_{coll}-scaling.

The detailed evolution of the spectra from peripheral to central events is shown in Fig. 3, for the six centrality bins. Each spectrum has been been divided by $\langle N_{part}/2\rangle$ and a fit to the data for the most peripheral bin. N_{part}-scaling would correspond to the ratio being constant at one (solid line), whereas N_{coll}-scaling, shown by the dashed line, would lead to an increase by a factor of two from peripheral to central events. Again, the brackets show the systematic uncertainty (90% C.L.). It is remarkable that the change in spectral shape over this range of centralities is small compared to that between $p + \bar{p}$ collisions and peripheral events shown in the top panel of Fig. 2. In particular at $p_T > 3$ GeV/c, the data scale with the number of participants to very good approximation.

The scaling behaviour in various regions of p_T is further illustrated in Fig. 4. Here we show the yield per participant pair in six bins of p_T between 0.45 and 4.25 GeV/c, normalized to the yield per participant pair in the most peripheral bin. The expectation for N_{coll}-scaling relative to the most peripheral bin is again shown as a dashed line. The observed evolution can be contrasted with the expectation that particle production should be characterized by a change from $\langle N_{part}\rangle$ scaling at low p_T to $\langle N_{coll}\rangle$ scaling at high p_T, with $\langle N_{part}\rangle$ increasing from 65 to 344 and $\langle N_{coll}\rangle$ from 107 to 1050 between the most peripheral collisions and the most central collisions studied here. No corresponding increase in particle production per participant at $p_T = 3$ GeV/c and above is observed. Rather, the yields in this region scale approximately with the number of participating nucleons.

The failure of binary collision scaling at intermediate

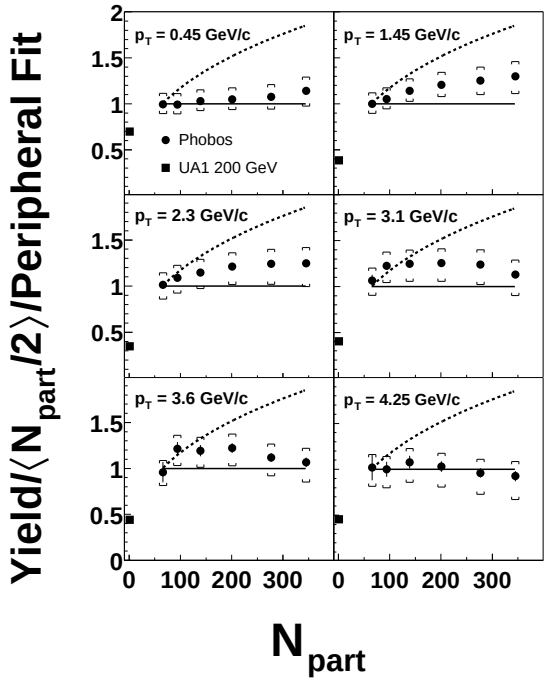

FIG. 4: Charged hadron yields per participant pair in 6 different transverse momentum bins, plotted as a function of N_{part}. The data are normalized to the yield in the most peripheral centrality bin. The dashed (solid) line shows the expectation for N_{coll} (N_{part}) scaling from peripheral to central collisions. The brackets indicate the systematic uncertainty for the centrality evolution of this ratio (90% C.L.).

and large p_T was previously observed in Au+Au collisions at $\sqrt{s_{NN}} = 130$ GeV [7]. This effect has been interpreted as the result of the energy loss of jets in the dense medium, leading to a suppression of leading hadrons relative to the expected scaling. The observed particle spectra are believed to depend on a complex interplay of initial and final state effects in the production and fragmentation of high p_T partons, including initial state multiple scattering, nuclear shadowing and parton energy loss. Our observations show that, surprisingly, the combination of all effects leads to an apparently very simple centrality scaling at large p_T, providing a challenge to theoretical descriptions. That this is not accidental is suggested by the agreement with earlier measurements at $\sqrt{s_{NN}} = 130$ GeV. The lower energy data [17, 18], when compared over the same centrality range, show very similar centrality scaling, even though the invariant yield at high p_T increases much more rapidly with increasing beam energy than the overall particle yield. It has recently been argued that the observed scaling could be naturally explained in a model assuming the dominance of surface emission of high-p_T hadrons [19]. However, the approximate participant scaling has also been explained in the context of initial state saturation models [20]. Experimentally, upcoming studies of d+Au collisions at RHIC will provide further insight into the modification of particle spectra in a nuclear environment.

This work was partially supported by U.S. DOE grants DE-AC02-98CH10886, DE-FG02-93ER40802, DE-FC02-94ER40818, DE-FG02-94ER40865, DE-FG02-99ER41099, and W-31-109-ENG-38 as well as NSF grants 9603486, 9722606 and 0072204. The Polish group was partially supported by KBN grant 2-P03B-10323. The NCU group was partially supported by NSC of Taiwan under contract NSC 89-2112-M-008-024.

[1] See e. g. J. P. Blaizot, Nucl. Phys. **A661** (1999) 3.
[2] See e. g. T. Sjostrand, Pythia manual, Comp. Phys. Comm. **82** (1994) 74.
[3] K. Adcox *et al.*, Phys. Rev. Lett. **86** (2001) 3500.
[4] B. B. Back *et al.*, Phys. Rev. **C65** (2002), 061901.
[5] D. Kharzeev and E. Levin, nucl-th/0108006
[6] M. Gyulassy and M. Plümer, Phys. Lett. **243**, (1990) 432.
[7] K. Adcox *et al.*, Phys. Rev. Lett. **88** (2002) 022301.
[8] M. Gyulassy *et al.*, Nucl. Phys. **A698** (2002) 631.
[9] B. B. Back *et al.*, Phys. Rev. Lett. **88** (2002) 022302.
[10] B. B. Back *et al.*, Nucl. Phys. **A661** (1999) 690.
[11] H. Pernegger *et al.*, Nucl. Instrum. Methods. **A419** (1998) 549.
[12] B. B. Back *et al.*, Nucl. Phys. **A698** (2002) 416.
[13] B. B. Back *et al.*, Phys. Rev. Lett. **85** (2000) 3100.
[14] M. Gyulassy and X. N. Wang, Comp. Phys. Comm. **83** (1994) 307. We used HIJING V1.35 with standard parameter settings.
[15] B. B. Back *et al.*, arXiv:nucl-ex/0206012, Phys. Rev. **C** in press.
[16] C. Albajar *et al.*, Nucl. Phys. **B335**, (1990) 261.
[17] C. Adler *et al.*, Phys. Rev. Lett. **89** (2002) 202301.
[18] K. Adcox *et al.*, arXiv:nucl-ex/0207009.
[19] B. Müller, Duke preprint DUKE-TH-02-225, arXiv:nucl-th/0208038.
[20] D. Kharzeev, E. Levin, L. McLerran, BNL preprint BNL-NT-02/22, arXiv:hep-ph/0210332